

THE NUCLEON SPIN STRUCTURE FROM LATTICE QCD*

CONSTANTIA ALEXANDROU^{a,b}, MARTHA CONSTANTINOUC^c
KYRIAKOS HADJIYIANNAKOU^b, KARL JANSEN^d, CHRISTOS KALLIDONIS^e
GIANNIS KOUTSOUB^b, ALEJANDRO VAQUERO AVILÉS-CASCO^f

^aDepartment of Physics, University of Cyprus
P.O. Box 20537, 1678 Nicosia, Cyprus

^bThe Cyprus Institute, 20 Kavafi Str., Nicosia 2121, Cyprus

^cDepartment of Physics, Temple University, Philadelphia, PA 19122-1801, USA

^dNIC, DESY, Platanenallee 6, 15738 Zeuthen, Germany

^eDepartment of Physics and Astronomy, Stony Brook University
Stony Brook, NY 11794, USA

^fDepartment of Physics and Astronomy, University of Utah
Salt Lake City, UT 84112, USA

(Received March 5, 2019)

We evaluate the nucleon spin decomposition to quarks and gluons contributions using lattice QCD. One ensemble of maximally twisted mass fermions with two degenerate light quarks tuned to reproduce the physical value of the pion mass has been analyzed. State-of-the-art techniques have been employed to increase the statistical accuracy of sea quarks contributions. Both spin and momentum sum rules are found to be satisfied within the statistical and systematic uncertainty.

DOI:10.5506/APhysPolBSupp.12.861

1. Introduction

The nucleon spin puzzle was triggered in 1987 when the European Muon Collaboration [1] measured a very small contribution, compatible with zero, from the quarks to the nucleon spin. Recent experiments measure about 30% contribution [2] to the nucleon spin from quarks and there are indications for a significant gluon contribution [3]. Since the spin of the nucleon should emerge from the quark–gluon and the gluon–gluon interactions, a first principles calculation is highly desirable. In this work, we perform lattice QCD simulations using maximally twisted mass fermions with two dynamical mass degenerate light quarks with masses tuned to reproduce

* Presented by K. Hadjiyiannakou at the Diffraction and Low- x 2018 Workshop, August 26–September 1, 2018, Reggio Calabria, Italy.

the physical pion mass. On the lattice, the contribution of the valence quarks has been measured in high precision but a complete decomposition of the nucleon should include also disconnected contributions from the sea quarks and the gluons. Disconnected diagrams are typically noisy because are susceptible to vacuum fluctuations, therefore, special techniques should be employed in combination with a large statistics to tame the error leading to an increased computational cost. With the help of recent algorithmic developments combined with the computational power provided by the GPUs enabled us to accurately determine all the contributions involved in order to provide a complete picture of both spin and momentum decomposition. For other studies, the interested reader is referred to Ref. [4].

2. Extraction of the nucleon matrix elements on the lattice

2.1. Nucleon matrix elements

In the literature, two approaches have been suggested to decompose the nucleon spin. One gauge-invariant way introduced by Ji [5], namely

$$J_N = \sum_q J_q + J_g = \sum_q \left(\frac{1}{2} \Delta \Sigma_q + L_q \right) + J_g, \quad (1)$$

where $\frac{1}{2} \Delta \Sigma_q$ is the intrinsic quark spin, L_q is the quark orbital angular momentum and J_g is the total gluon angular momentum. In Ji's decomposition, the gluon contribution cannot decompose further. In contrast, the Jaffe–Manohar decomposition [6] given as

$$J_N = \sum_q \left(\frac{1}{2} \Delta \Sigma_q + \mathcal{L}_q \right) + L_g + \Delta G \quad (2)$$

decomposes the gluon contribution to an orbital angular momentum L_g and intrinsic polarization ΔG . Note that $L_q \neq \mathcal{L}_q$, thus the quark orbital angular momentum is different in the two decompositions. For the physical meaning and the gauge invariance issue of the Jaffe–Manohar decomposition, see Ref. [7].

In this study, we employ Ji's decomposition. The intrinsic quark spin is the axial charge of the nucleon, up to a factor of 2, which can be computed directly on the lattice from the nucleon axial-vector matrix element. The total quark contribution J_q is expressed through the Generalized Form Factors (GFFs) at zero momentum transfer as $J_q = \frac{1}{2} (A_{20}^q(0) + B_{20}^q(0))$, where $A_{20}^q(Q^2)$ and $B_{20}^q(Q^2)$ are extracted from the nucleon matrix element of the vector one-derivative operator. For the computation of the gluon contribution J_g , we employ the gluon operator [8] $\mathcal{O}_g^{\mu\nu} = 2\text{Tr} [G_{\mu\sigma} G_{\nu\sigma}]$

with $G_{\mu\nu}$ the field strength tensor. We take the traceless combination giving the scalar operator $\mathcal{O}_B = \mathcal{O}_{44} - \frac{1}{3}\mathcal{O}_{jj}$, and from the matrix element $\langle N|\mathcal{O}_B|N\rangle = -2m_N\langle x\rangle_g$, one can extract $A_{20}^g(0) = \langle x\rangle_g$. To compute $J_g = \frac{1}{2}[A_{20}^g(0) + B_{20}^g(0)]$, $B_{20}^g(0)$ is also needed, but assuming that spin and momentum sums are satisfied, one can relate B_{20} of gluons to quarks such as $\sum_q B_{20}^q(0) = -B_{20}^g(0)$.

2.2. Correlation functions

In order to extract the nucleon matrix elements from the correlation functions, we analyze one gauge ensemble of two mass degenerate twisted mass fermions with a clover term with mass tuned in order to approximately reproduce the physical pion mass. The lattice volume is $48^3 \times 96$ with lattice spacing $\alpha = 0.0938(3)$ fm [9]. For the strange quark, we use Osterwalder–Seiler fermions where the strange quark mass is tuned to reproduce the physical Ω^- mass.

The three-point correlation function receives contribution from two types of diagrams. In the connected diagram, the insertion operator couples directly to a valence quark, whereas in the disconnected diagram, the insertion operator couples to a sea quark, and the coupling to the nucleon propagator is mediated through the gauge background. The connected diagram can be computed using standard approaches, such as sequential inversions through the sink, giving the dominant contribution. The computation of the disconnected diagram is significantly more complicated because, on the one hand, it involves the quark loop which is notoriously expensive to compute and, on the other, needs the nucleon propagator for large number of source positions to control the statistical error.

Since the simulation is performed directly on a physical ensemble, conventional solvers such as the conjugate gradient (CG) method face a critical slow down as the condition number of the Dirac operator increases dramatically. In order to overcome this delicate point, we deflate the lowest 500 modes of the square twisted mass operator to speedup the inversions. For the estimation of the quark loop, we follow stochastic approaches such as the one-end trick which provides an increased signal-to-noise ratio. For the strange quark, we also employ the Truncated Solver Method (TSM) [10]. For the computation of the gluon loops, we perform stout smearing on the gauge links of the gluon operator to smooth UV fluctuations. The nucleon propagator has been computed for 100 source positions to control statistical uncertainty in the disconnected diagrams.

We renormalize our lattice results using the RI'-MOM scheme and subtract lattice artifacts using lattice perturbation theory. For details, see Ref. [11]. The renormalization of the gluon operator is carried out perturbatively as explained in Ref. [8]. Results are given in $\overline{\text{MS}}$ -scheme at 2 GeV.

3. Results

Our results for the intrinsic quark spin of the up, down and strange ones are shown in Fig. 1 as a function of the pion mass, comparing with other studies. Focusing on the simulation directly at the physical point, we observe that the contribution of the disconnected diagrams is crucial in order to find agreement with the experimental results. An additional point that one can make from Fig. 1 is that there is not a significant pion mass dependence. From Fig. 1, we can also conclude that quenching effects are negligible since $N_f = 2$ and $N_f = 2+1+1$ are in perfect agreement.

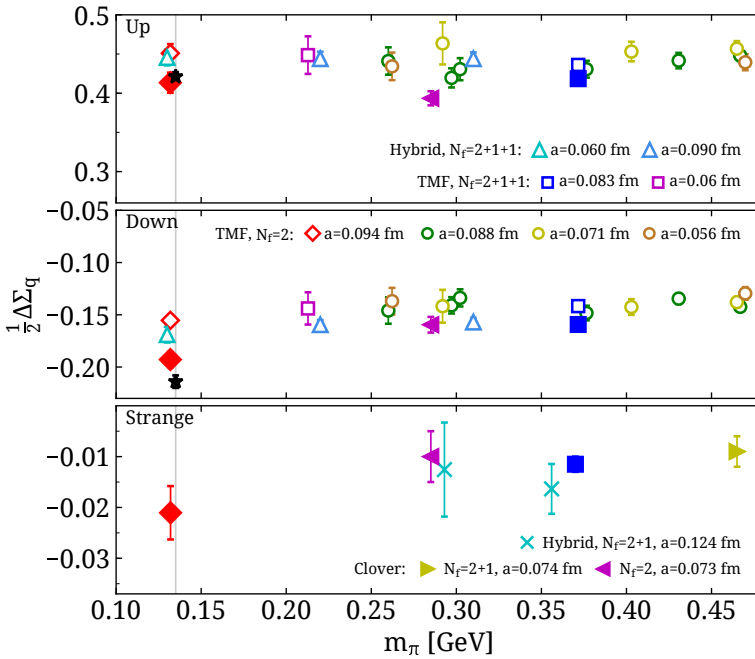


Fig. 1. (Color online) The up (upper), down (center) and strange (lower) quark intrinsic spin contributions to the nucleon spin *versus* the pion mass. Open symbols show results with only connected contributions, while filled symbols results including disconnected ones. Gray/red diamonds are the results of this work. Results from other studies are also presented.

The results for the nucleon spin and momentum decomposition are shown in Fig. 2 [8]. The disconnected diagrams have a significant contribution, and we find that both the spin and momentum sums are satisfied within the errors. Results are summarized in Table I.

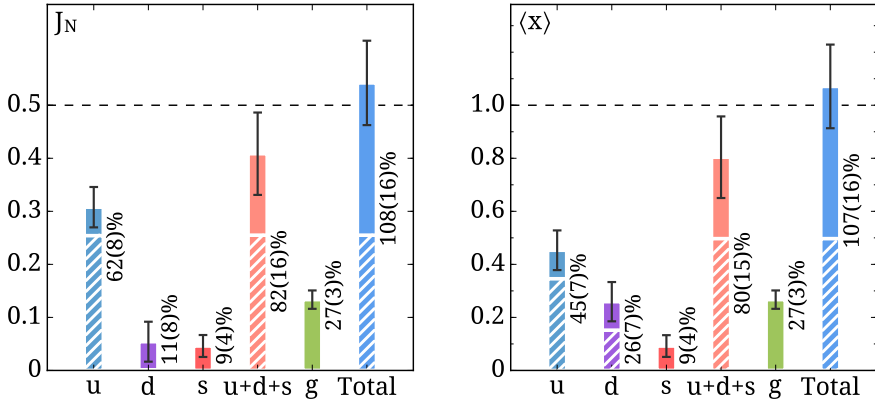


Fig. 2. Left: Nucleon spin decomposition. Right: Nucleon momentum decomposition. The striped segments show valence quark contributions (connected) and the solid segments the sea quark and gluon contributions (disconnected). Results are given in $\overline{\text{MS}}$ scheme at 2 GeV.

TABLE I

Our results for the intrinsic spin ($\frac{1}{2}\Delta\Sigma$), angular (L) and total (J) momentum contributions to the nucleon spin and to the nucleon momentum $\langle x \rangle$, from quarks and gluons, where the first error is statistical and the second a systematic due to excited states.

	$\frac{1}{2}\Delta\Sigma$	J	L	$\langle x \rangle$
u	0.415(13)(2)	0.308(30)(24)	-0.107(32)(24)	0.453(57)(48)
d	-0.193(8)(3)	0.054(29)(24)	0.247(30)(24)	0.259(57)(47)
s	-0.021(5)(1)	0.046(21)(0)	0.067(21)(1)	0.092(41)(0)
g	—	0.133(11)(14)	—	0.267(22)(27)
tot.	0.201(17)(5)	0.541(62)(49)	0.207(64)(45)	1.07(12)(10)

4. Conclusion

This study presents a complete calculation of the nucleon spin and momentum based on Ji's decomposition. One $N_f = 2$ twisted mass ensemble at the physical point has been analyzed. The sea quarks contributions are evaluated using state-of-the-art techniques with unprecedented accuracy. For the intrinsic quark spin we find $\frac{1}{2}\Delta\Sigma_{u+d+s} = 0.201(17)(5)$ for the nucleon spin $J_N = 0.541(62)(49)$ and for the momentum sum $\sum_q \langle x \rangle_q + \langle x \rangle_g = 1.07(12)(10)$.

REFERENCES

- [1] J. Ashman *et al.* [European Muon Collaboration], *Phys. Lett. B* **206**, 364 (1988).
- [2] C.A. Aidala, S.D. Bass, D. Hasch, G.K. Mallot, *Rev. Mod. Phys.* **85**, 655 (2013) [arXiv:1209.2803 [hep-ph]].
- [3] I. Nakagawa, [PHENIX Collaboration], *EPJ Web Conf.* **141**, 03006 (2017).
- [4] Y.-B. Yang *et al.*, *Phys. Rev. D* **98**, 074506 (2018) [arXiv:1805.00531 [hep-lat]].
- [5] X.-D. Ji, *Phys. Rev. Lett.* **78**, 610 (1997) [arXiv:hep-ph/9603249].
- [6] R.L. Jaffe, A. Manohar, *Nucl. Phys. B* **337**, 509 (1990).
- [7] M. Wakamatsu, *Phys. Rev. D* **94**, 056004 (2016) [arXiv:1607.04018 [hep-ph]].
- [8] C. Alexandrou *et al.*, *Phys. Rev. D* **96**, 054503 (2017) [arXiv:1611.06901 [hep-lat]].
- [9] A. Abdel-Rehim *et al.* [ETM Collaboration], *Phys. Rev. D* **95**, 094515 (2017) [arXiv:1507.05068 [hep-lat]].
- [10] G.S. Bali, S. Collins, A. Schafer, *Comput. Phys. Commun.* **181**, 1570 (2010) [arXiv:0910.3970 [hep-lat]].
- [11] C. Alexandrou *et al.*, *Phys. Rev. D* **96**, 054507 (2017) [arXiv:1705.03399 [hep-lat]].